Novel Many-objective NSGA-FA Algorithm to Minimize Fuel Cost, Power Loss and Emission of Electric Systems

Gang Guo, Jie Qian*, and Shuaiyong Li

Abstract—**Increasingly mature computer technology is very conducive to solve the complex optimizations of power system. To effectively deal with the many-objective optimal power flow (MOOPF) problems, a novel NSGA-FA algorithm which alleviates the limitation of local optimum is put forward in this paper. The NSGA-FA algorithm combines the special sorting rule of non-dominated sorting genetic algorithm-III (NSGA-III) and the location-updating mechanism of many-objective firefly algorithm (MFA). Furthermore, the optimal elite guidance (E_{-guide}) mechanism and the non-duplicate elite solution storage (*NDES*) strategy are proposed to optimize operation-efficiency and solution-diversity of NSGA-FA algorithm. The applicability and preponderance of NSGA-FA algorithm compared with NSGA-III and MFA methods are evaluated by both bi-objective and tri-objective MOOPF experiments on IEEE 30-bus and 57-bus systems. Furthermore, the hyper-volume (HV) metric and the detailed results of five simulation trials intuitively indicate that the presented NSGA-FA algorithm achieves the more preferable Pareto front (PF) with superior-diversity and fast-convergence. In general, the suggested NSGA-FA algorithm provides an innovative idea for the application of computer technology on the economic operation of electric systems.**

Index Terms—**NSGA-FA algorithm, Many-objective optimal power flow, Computer technology, Optimal elite guidance mechanism**

I. Introduction

THE stable operation of electric system, one of the most widely-used energies, is necessary to maintain people's daily lives. The optimal operation of power systems involves multiple practical problems such as the hydro-thermal unit commitment [1], the economic load dispatch [2] and the design of fuzzy sliding mode controller for hydraulic turbine regulating system [3].

Manuscript received November 7, 2019; revised May 15, 2020. This work was supported the National Natural Science Foundation Project of China (No.61703066), Natural Science Foundation Project of Chongqing (No.cstc2018jcyjAX0536).

Gang Guo is with the School of Information Technology, Luoyang Normal University, Luoyang, Henan 471934, China (e-mail: guogangchina @sina.cn).

Jie Qian is with the Key Laboratory of Complex Systems and Bionic Control, Chongqing University of Posts and Telecommunications, Chongqing 400065, China (corresponding author, Tel: 13618344186; e-mail: qianjie@126.com).

Shuaiyong Li is with the Key Laboratory of Industrial Internet of Things & Networked Control, Ministry of Education, Chongqing University of Posts and Telecommunications, Chongqing 400065, China (e-mail: lishuaiyong@cqupt.edu.cn).

The many-objective optimal power flow (MOOPF), as an important means to improve the power-quality, is a minimum optimization problem with two or more objective functions [4-7]. However, the typical characteristics of non-convexity and non-differentiability make traditional methods unsuitable for solving the MOOPF problems. The maturity of computer technology makes intelligent algorithms such as the quasi-oppositional cuckoo search algorithm [8], the improved NSGA-III algorithm [9] and the hybrid bat algorithm [10] can solve the MOOPF problems successfully.

A. *Major Contributions*

The firefly algorithm with easily-adjustable parameters is derived from the natural behaviors and has been applied in many practical optimization fields [11-13]. The research shows that the many-objective firefly algorithm (MFA) is capable to deal with MOOPF problems [14, 15]. But it is easily limited by local optimums and still has room for improvement. Simulation trials in this paper indicate that the non-dominated sorting genetic algorithm-III (NSGA-III), the commonly-used comparison standard of multi-objective algorithms, can also handle the MOOPF problems with poor performance. To handle with the non-liner MOOPF problems more effectively, the non-dominated sorting genetic-modified firefly (NSGA-FA) algorithm which is inspired by NSGA-III and MFA algorithms is proposed in this paper.

As one of major contributions, the NSGA-FA algorithm integrates the unique sorting strategy of NSGA-III algorithm and the brightness-based location updating mode of MFA algorithm. Besides, the optimal elite guidance (E_{-guide}) mechanism and the nonlinear adjustment weight (ω_{non}) coefficient are put forward to optimize the population diversity and global-searching capability of NSGA-FA algorithm. Furthermore, the non-duplicate elite solution storage (*NDES*) strategy which improves the optimizing efficiency is also presented to retain the high-quality power flow solutions.

Based on five MOOPF experiments on IEEE 30-bus and 57-bus systems, the great advantages of NSGA-FA algorithm comparing with NSGA-III and MFA methods in seeking the evenly-distributed Pareto front (PF) and better compromise solution (BCS) are powerfully verified.

B. *Content and Structure*

The main content and structure of this paper are set as follows. Section II gives the mathematical model of MOOPF problems including the multiple constraints and optimal goals. The proposed NSGA-FA algorithm and major improvements are described in Section III. The non-inferior sorting rule and *NDES* strategy which aim to seek the satisfactory Pareto optimal set (POS) are also shown in Section III. Then, Section IV introduces the standard IEEE 30-bus and 57-bus systems, as well as the detailed parameter settings of three involved algorithms. Section V gives the simulation results of all bi-objective and tri-objective MOOPF experiments. And in Section VI, the performance of NSGA-FA algorithm in dealing with MOOPF problems compared with MFA and NSGA-III methods is evaluated based on the convergence, computational complexity and PF-diversity. Finally, the conclusions are given in Section VII.

II. MOOPF Model

Two major parts, strict constraints and optimal goals, constitute the mathematical model of MOOPF problems.

A. System Constraints

The MOOPF problems are limited by equality constraints (*EC*s) and inequality constraints (*IC*s). Two *EC*s shown in (1) and (2) are essentially the power balance equations of electrical systems [14, 16]. The *IC*s are usually divided into the *IC*s on control variables and the *IC*s on state ones.

$$P_{Gi}-P_{Di}-V_i\sum_{j\in N_i}V_j(G_{ij}\cos\delta_{ij}+B_{ij}\sin\delta_{ij})=0, i\in N \quad (1)$$

$$\begin{aligned}&Q_{Gi}-Q_{Di}-V_i\sum_{j\in N_i}V_j(G_{ij}\sin\delta_{ij}-B_{ij}\cos\delta_{ij})=0\\&i\in N_{PQ}\ \delta_{ij}=\delta_i-\delta_j\end{aligned} \quad (2)$$

1) ICs on Control Variables

The control variables of MOOPF problems, also called independent variables, are composed of the generator active power output at PV node (P_G), generator node voltage (V_G), tap ratios of transformer (T) and reactive power injection (Q_C) [17, 18]. In detail, the *IC*s on control variables are summarized as (3)~(6).

$$P_{Gi}^{\max}\ge P_{Gi}\ge P_{Gi}^{\min}, i\in N_G (i\neq 1) \quad (3)$$

$$V_{Gi}^{\max}\ge V_{Gi}\ge V_{Gi}^{\min},\ i\in N_G \quad (4)$$

$$T_i^{\max}\ge T_i\ \ge T_i^{\min},\ i\in N_T \quad (5)$$

$$Q_{Ci}^{\max}\ge Q_{Ci}\ge Q_{Ci}^{\min},\ i\in N_C \quad (6)$$

2) ICs on State Variables

The state variables of MOOPF problems are composed of the generator active power at slack node (P_{G1}), load node voltage (V_L), generator reactive power (Q_G) and apparent power of transmission line (S) [10, 19]. Then, the *IC*s on state variables are represented as (7)~(10).

$$P_{G1}^{\max}\ge P_{G1}\ge P_{G1}^{\min} \quad (7)$$

$$V_{Li}^{\max}\ge V_{Li}\ge V_{Li}^{\min},\ i\in N_{PQ} \quad (8)$$

$$Q_{Gi}^{\max}\ge Q_{Gi}\ge Q_{Gi}^{\min},\ i\in N_G \quad (9)$$

$$S_l^{\max}-S_l\ge 0,\ l\in N_L \quad (10)$$

The meaning of above special symbolic is clarified in literatures [10, 18, 20].

B. Control Variables Processing

The Newton-Raphson method, which takes two above *EC*s as the termination condition of power flow calculation, is adopted in this paper. The processing strategies of control and state variables that violate *IC*s are the key points of this paper.

In the initialization phase, these control variables that do not satisfy the *IC*s (3)~(6) can be modified based on Formula (11).

$$C_i=\begin{cases}C_i^{\max} & if\ C_i>C_i^{\max}\\ C_i^{\min} & if\ C_i<C_i^{\min}\end{cases} \quad (11)$$

where C_i indicates the *i*th control variable set which is limited within the valid range of [C_i^{min}, C_i^{max}].

C. State Variables Processing

Innovatively, an effective constraint-priority strategy of processing the state variables is put forward in this paper. The power flow solution whose corresponding state variable set has smaller constraint-violation (*Cvio*) value will be assigned a higher adoption-priority. The *Cvio* value can be calculated as (12).

$$Cvio(S_i)=\sum_g \max(IC_g(S_i,C_i),0) \quad (12)$$

where S_i is the *i*th state variable set and g is the number of *IC*s on state variables.

The adoption-priority of each power flow solution is defined based on Formulas (13) and (14). It can be determined that the *p*th power flow solution is superior to the *q*th one when condition (13) or (14) is satisfied

$$Cvio(p)<Cvio(q) \quad (13)$$

$$\begin{cases}Cvio(p)=Cvio(q)\\ Ob_i(S_p,C_p)\le Ob_i(S_q,C_q),\forall i\in\{1,2,...,M\}\\ Ob_j(S_p,C_p)<Ob_j(S_q,C_q),\exists j\in\{1,2,...,M\}\end{cases} \quad (14)$$

where $Ob_i(S_p,C_p)$ is the *i*th goal value of the *p*th solution. M is the number of goals for simultaneous optimization.

D. Optimal Goals

The optimizations of emission (*Em*), the basic fuel cost (*Fc*), the fuel cost with valve-point effect (Fc_v) and the active power loss (*Pl*) are considered in this paper. The four mentioned goals are shown as (15)~(18).

◆ *Em* (ton/h)

$$Em=\sum_{i=1}^{N_G}[\alpha_i P_{Gi}^2+\beta_i P_{Gi}+\gamma_i+\eta_i\exp(\lambda_i P_{Gi})] \quad (15)$$

◆ *Fc* ($/h)

$$Fc=\sum_{i=1}^{N_G}(a_i+b_iP_{Gi}+c_iP_{Gi}^2) \quad (16)$$

◆ Fc_v ($/h)

$$\begin{aligned}Fc_v=&\sum_{i=1}^{N_G}(a_i+b_iP_{Gi}+c_iP_{Gi}^2+\\&\left|d_i\times\sin(e_i\times(P_{Gi}^{\min}-P_{Gi}))\right|)\end{aligned} \quad (17)$$

◆ *Pl* (MW)

$$Pl=\sum_{k=1}^{N_L}c_k[V_i^2+V_j^2-2V_iV_j\cos(\delta_i-\delta_j)] \quad (18)$$

The meaning of special symbolic can be found in the literatures [10, 21, 22].

III. Algorithms

The classical NSGA-III, MFA methods and the novel

NSGA-FA algorithm proposed in this paper are used to handle the strictly-constrained MOOPF problems.

A. Comparison Algorithms

In essence, the presented NSGA-FA algorithm is the combination and improvement of NSGA-III and MFA algorithms. Besides, NSGA-III method is often adopted as the comparison cornerstone to evaluate the performance of new many-objective algorithms. Although the NSGA-III method has unsatisfactory performance in dealing with MOOPF problems, its unique non-inferior sorting strategy provides an excellent inspiration for NSGA-FA algorithm.

The MFA algorithm has broad application prospects due to the easily-adjust parameters and good-robustness. It also provides the main body and great inspiration for the suggested NSGA-FA algorithm to handle MOOPF problems.

In this paper, both NSGA-III and MFA are chosen as comparison algorithms to verify the applicability and superiority of novel NSGA-FA algorithm.

B. NSGA-FA Algorithms

The detailed description of standard MFA algorithm can be found in literatures [14, 23, 24]. Based on MFA algorithm, two major improvements are integrated into the presented NSGA-FA algorithm.

1) E_{-guide} Mechanism

The E_{-guide} mechanism based on the current best solution (op_{best}) is proposed to modify the location (L_{oca}) updating model of NSGA-FA method. It is conducive to quicken the speed of firefly population approaching to the ultimate op_{best} solution. The improved L_{oca}^{new} with E_{-guide} mechanism is defined as (19).

$$\begin{aligned} L_{oca(i)}^{new} &= L_{oca(i)} + \delta_0 \exp(-\gamma r_{ibest}^2)(op_{best} - L_{oca(i)}) \\ &\quad + \rho * \xi_i \ , \forall i \in \{1, 2, \cdots N\} \end{aligned} \tag{19}$$

where δ_0 is the attractiveness at r_{ibest}=0 and ρ indicates the randomization parameter. ξ_i is a D-dimensional random vector which satisfies the uniform distribution. The r_{ibest}, the distance between the ith solution and the op_{best} one, can be calculated based on (20).

$$r_{ibest} = \|C_i - C_{best}\| = \sqrt{\sum_{k=1}^{D} (C_{i,k} - C_{best,k})^2} \tag{20}$$

2) Nonlinear ω_{non} Coefficient

To optimize the diversity of NSGA-FA algorithm, a nonlinear ω_{non} coefficient is incorporated into the L_{oca}^{new} updating formula (21). The ω_{non} coefficient is limited within [ω_{min}, ω_{max}] and it is renovated according to Equation (22) during the iteration.

$$\begin{aligned} L_{oca(i)}^{new} &= \omega_{non} L_{oca(i)} + \delta_0 \exp(-\gamma r_{ibest}^2)(op_{best} - L_{oca(i)}) \\ &\quad + \rho * \xi_i \quad \forall i \in \{1, 2, \cdots N\} \end{aligned} \tag{21}$$

$$\begin{aligned} \omega_{non}(i) &= \omega_{\max} - \theta_1(\omega_{\max} - \omega_{\min}) + \\ &\quad \theta_2(\omega(i-1) - (\omega_{\max} + \omega_{\min}) / 2) \end{aligned} \tag{22}$$

where θ_1 and θ_2 are two random numbers which belong to (0,1).

The nonlinear adjustment of ω_{non} coefficient is efficient to avoid the premature convergence caused by poor-diversity in the iterative late.

C. POS Selection Strategy

To seek high-quality POS from the reserved non-inferior solution (*RES*) set, the classical sorting rule proposed by Deb Kalyanmoy [25-27] and the novel *NDES* storage strategy are applied on MOOPF problems.

1) NDES Storage Strategy

In order to preserve the elite solutions as much as possible, the *RES* set contains not only the *N* power flow solutions generated by Formula (21) at the *i*th iteration, but also the *N* solutions obtained at the (*i*-1)th iteration. The *NDES* storage strategy, which is helpful to reduce the computational complexity, removes duplicate solutions from the *RES* set. In principle, the *RES* set is consisted of N_{res} ($N \leqslant N_{res} \leqslant 2N$) alternative solutions.

2) Non-inferior Sorting Rule

The non-inferior sorting rule aims to seek the satisfactory POS with size of *N* from the *RES* set. It is organized as follows.

Step 1: Based on the dominance principles (13) and (14), these power flow solutions with *rank*=1 which are not dominated by any other solutions of *RES* set are determined.

Step 2: Remove the elite solutions with *rank*=1, and assign these suboptimal solutions which are not dominated by the rest solutions of *RES* set as *rank*=2 based on the same dominance rule.

Step 3: Repeat the above operation until all N_{res} solutions have corresponding *rank* value.

In order to clarify the dominant relationship of two power flow solutions with the same *rank* index, the crowding distance (*cdis*) that can measure the distribution-uniformity is adopted. The smaller value of *cdis* represents the denser distribution of solution set. The *cdis* index of *i*th solution is defined as (23) [25].

$$cdis(i) = \sum_{j=1}^{N} \frac{Ob_j(i-1) - Ob_j(i+1)}{Ob_j^{\max} - Ob_j^{\min}} \tag{23}$$

where Ob_j^{min} and Ob_j^{max}, respectively, are the minimum and maximum of the *j*th goal.

The power flow solutions satisfying condition (24) or (25) will be assigned the higher adoption priority. These solutions which rank in the top *N* are the ultimate POS set determined by the proposed non-inferior sorting rule and *NDES* storage strategy.

$$rank(i) < rank(j) \tag{24}$$

$$\begin{cases} rank(i) = rank(j) \\ cdis(i) > cdis(j) \end{cases} \tag{25}$$

D. NSGA-FA Algorithm on MOOPF

The necessary correspondence relations are clarified to understand the combination and application of NSGA-FA algorithm on MOOPF problems. Each firefly is essentially a 24-dimensional control variable set of IEEE 30-bus system and a 33-dimensional control variable set of IEEE 57-bus system. The firefly individual with best-brightness named as op_{best} indicates the power flow solution with maximum satisfaction (*sat*). The calculation of *sat* value is expressed as (27) and the details can be found in literatures [18, 24].

The pseudo codes of solving MOOPF problems by NSGA-FA algorithm is shown in TABLE I.

$$s_i(k)=\begin{cases} 1 & f_i \le f_i^{\min} \\ \dfrac{Ob_i^{\max}-Ob_i}{Ob_i^{\max}-Ob_i^{\min}} & Ob_i^{\min} < Ob_i < Ob_i^{\max} \\ 0 & Ob_i \ge Ob_i^{\max} \end{cases} \tag{26}$$

$$k=1,2,\ldots N \quad i=1,2,\ldots,M$$

$$sat(k)=\frac{\sum_{i=1}^{M} s_i(k)}{\sum_{k=1}^{N}\sum_{i=1}^{M} s_i(k)} \tag{27}$$

IV. Systems and Parameters

To verify the practicability of NSGA-FA algorithm, the standard IEEE 30-bus and IEEE 57-bus systems are adopted for MOOPF simulation experiments. In addition, the relatively optimal combination of algorithm parameters is studied as well.

A. Power Systems

The structures of IEEE 30-bus and 57-bus systems are, respectively, shown in Fig. 1 and Fig. 2. The effective ranges of control variables and the fuel coefficients for the standard 30-bus system can be found in literatures [18, 28]. Besides, the detail of standard 57-bus system is clarified in literatures [18, 24].

Based on MATLAB 2014a software, both bi-objective and tri-objective MOOPF problems are studied on two different scale power systems. The five trials shown in TABLE II are performed on a PC with Intel(R) Core(TM) i5－7500 CPU @ 3.40 GHz with 8GB RAM.

B. Algorithm Parameters

The effect of ω_{non} coefficient on the optimization quality of NSGA-FA algorithm is studied. Fig. 3 gives the PFs with different ω_{non} ranges obtained by NSGA-FA, which clearly shows that the ω_{non} range of [0.90, 0.98] achieves the best PF.

Besides, the specific parameter settings of NSGA-III, MFA and NSGA-FA algorithms are given in TABLE III.

V. Simulation and Verification

Three bi-objective and two tri-objective simulation trials are carried out to test the performance of NSGA-III, MFA and NSGA-FA algorithms on MOOPF problems.

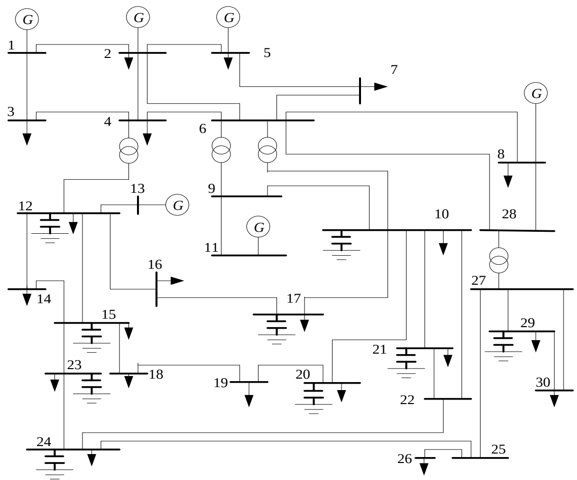

Fig.1. Structure of IEEE 30-bus system

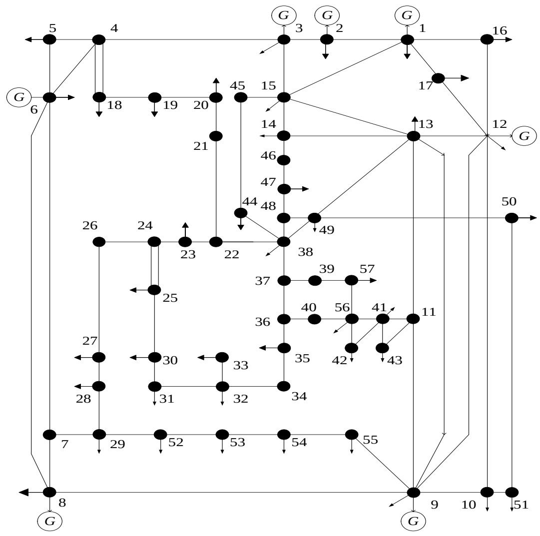

Fig.2. Structure of IEEE 57-bus system

A. Simulation on IEEE 30-bus System

Based on the two bi-objective and one tri-objective experiments which are performed on the IEEE 30-bus system, the availability of proposed NSGA-FA algorithm in solving MOOPF problem can be intuitively verified.

TABLE I

Pseudo Codes of NSGA-FA Algorithm

input: the randomly-generated *N D*-dimensional control variable sets and the parameters of NSGA-FA algorithm

begin

ite=1

Generate the initial *RES* set with 2*N* solutions at random;

Handle the unqualified control variable sets according to Formula (11);

while $ite < ite_{max}$

Update the location of firefly population based on (21);

Perform the power flow calculation based on the Newton-Raphson method;

Generate the *RES* set with N_{res} solutions based on the suggested *NDES* storage strategy;

Perform the non-inferior sorting operation based on *rank* and *cdis* values shown in (24) and (25) and determine the current POS set;

Select the current op_{best} solution with highest *sat* value based on (27);

ite=*ite*+1;

end while

end

output: the ultimate POS set and op_{best} solution

1) Exp 1: Simultaneous Optimization of Pl and Fc

Firstly, the *Pl* and *Fc* goals are optimized at the same on the IEEE 30-bus system. The PFs achieved by NSGA-III, MFA and NSGA-FA algorithms are given in Fig. 4. It clearly states the NSGA-FA algorithm finds the evenly-distributed PF with better diversity than two comparison methods. Besides, TABLE IV gives the detailed control variables of three BCS solutions. The presented NSGA-FA algorithm obtains the BCS solution including 4.9749 MW of *Pl* and 833.8974 \$/h of *Fc* which dominates the ones of NSGA-III and MFA methods. Comparing with the BCS solutions found by the published MOBBA-CPNS and NSGA-II methods, the BCS solution of NSGA-FA algorithm is also more preferable.

2) Exp 2: Simultaneous Optimization of Pl and Fc_v

The fuel cost considering valve-point effect has obvious non-convex characteristic, which will inevitably increase the optimization difficulty. In *Exp* 2, the *Pl* and Fc_v are minimized concurrently. The PFs and control variables of *Exp* 2, respectively, are shown in Fig. 5 and TABLE V. Fig. 5 indicates that although all the three methods have sought the feasible PFs, NSGA-FA algorithm achieves the most ideal one than MFA and NSGA-FA methods. TABLE V shows that the BCS of NSGA-FA which includes 5.8620 MW of *Pl* and 859.70 \$/h of Fc_v is more advantageous than the BCS solutions obtained by NSGA-III and MFA algorithms. The superiority of suggested NSGA-FA in handling bi-objective optimization is more convictive based on the given BCS result of published MOFA-PFA algorithm.

3) Exp 3: Simultaneous Optimization of Em, Pl and Fc

Compared with the dual-objective optimizations, the tri-objective ones are more difficult. The *Em*, *Pl* and *Fc* are optimized in *Exp* 3. Fig. 6 which gives the obtained PFs clearly shows that NSGA-FA finds the best PF while the NSGA-III seeks the worst one. The details of BCS solutions obtained by three involved methods and the comparison result from literature [24] are clarified in TABLE VI.

The BCS of NSGA-FA, which is composed by 0.2121 ton/h of *Em*, 4.5558 MW of *Pl* and 863.79 \$/h of *Fc*, is better than the BCS of NSGA-III including 0.2133 ton/h of *Em*, 4.7366 MW of *Pl* and 867.13 \$/h of *Fc*. The BCS of NSGA-FA algorithm also surpasses the one of MFA method including 0.2122 ton/h of *Em*, 4.6916 MW of *Pl* and 865.41 \$/h of *Fc*. Although the BCS solution of NSGA-FA algorithm cannot directly dominate the one of MODFA algorithm, its *Fc* and *Em* values are significantly smaller.

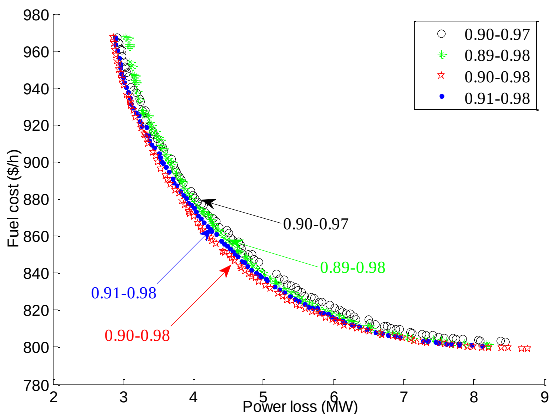

Fig.3. PFs with different ω_{non} of NSGA-FA algorithm

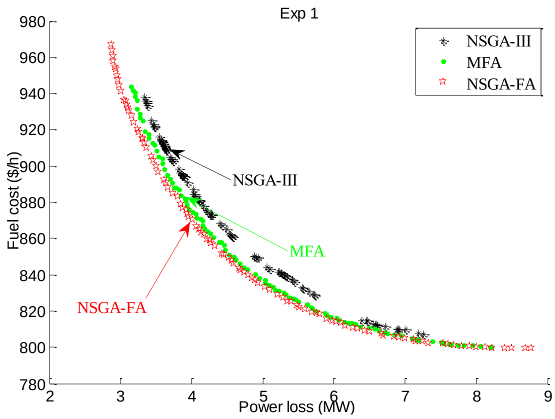

Fig.4. PFs of *Exp* 1

TABLE II
COMBINATION OF OPTIMIZATION GOALS

Goal	*Exp*1	*Exp*2	*Exp*3	*Exp*4	*Exp*5
Fc	*		*	*	*
Fc_v		*			
Pl	*	*	*	*	*
Em			*		*
IEEE 30-bus	✓	✓	✓		
IEEE 57-bus				✓	✓
Independent Repeat Experiment	30	30	30	30	30

TABLE III
PARAMETERS OF THREE ALGORITHMS

Parameters	NSGA-III	MFA	NSGA-FA
N	100	100	100
ite_{max}	300 (*Exp* 1 ~ *Exp* 3) 500 (*Exp* 4 ~ *Exp* 5)	300 (*Exp* 1 ~ *Exp* 3) 500 (*Exp* 4 ~ *Exp* 5)	300 (*Exp* 1 ~ *Exp* 3) 500 (*Exp* 4 ~ *Exp* 5)
mutation indictor/ percentage	20/1	-	-
crossover indictor/ percentage	20/0.1	-	-
number of divisions	10	-	-
δ_0	-	1	1
γ	-	1	1
ρ	-	0.1	0.1
ω_{min}	-	-	0.90
ω_{max}	-	-	0.98

TABLE IV
CONTROL VARIABLES OF *EXP* 1

Control Variables	NSGA-III	MFA	NSGA-FA	NSGA-II [24]	MOBBA-CPNS [29]
P_{G2}(MW)	59.3948	52.9686	53.1899	56.4213	52.1822
P_{G5}(MW)	34.2552	31.1296	31.1546	33.0438	32.7244
P_{G8}(MW)	33.7072	35.0000	34.9432	34.7867	35.0000
P_{G11}(MW)	24.7110	28.9024	28.2403	27.0643	26.9444
P_{G13}(MW)	19.6971	23.4827	23.8378	24.0395	23.7615
V_{G1}(p.u.)	1.0710	1.0970	1.0992	1.0955	1.1000
V_{G2}(p.u.)	1.0621	1.0843	1.0904	1.0824	1.0873
V_{G5}(p.u.)	1.0378	1.0618	1.0682	1.0557	1.0639
V_{G8}(p.u.)	1.0453	1.0734	1.0802	1.0713	1.0743
V_{G11}(p.u.)	1.0676	1.1000	1.0993	1.0822	1.1000
V_{G13}(p.u.)	1.0518	1.0986	1.0989	1.0657	1.0898
T_{11}(p.u.)	1.0276	0.9864	1.0493	0.9844	1.0193
T_{12}(p.u.)	0.9295	0.9234	0.9025	1.0316	0.9760
T_{15}(p.u.)	1.0217	0.9814	0.9873	1.0409	0.9834
T_{36}(p.u.)	0.9794	0.9634	0.9768	0.9980	0.9842
Q_{C10}(p.u.)	0.0328	0.0067	0.0400	0.0008	0.0404
Q_{C12}(p.u.)	0.0227	0.0423	0.0435	0.0271	0.0419
Q_{C15}(p.u.)	0.0267	0.0104	0.0407	0.0499	0.0131
Q_{C17}(p.u.)	0.0267	0.0069	0.0475	0.0226	0.0031
Q_{C20}(p.u.)	0.0445	0.0438	0.0364	0.0306	0.0111
Q_{C21}(p.u.)	0.0278	0.0060	0.0476	0.0122	0.0492
Q_{C23}(p.u.)	0.007	0.0242	0.0386	0.0253	0.0409
Q_{C24}(p.u.)	0.0101	0.0104	0.0372	0.0220	0.0373
Q_{C29}(p.u.)	0.0400	0.0235	0.0421	0.0075	0.0408
Pl (MW)	5.4485	5.0873	**4.9749**	5.0121	5.0223
Fc ($/h)	836.0571	834.6263	**833.8974**	838.9980	834.6417

TABLE V
CONTROL VARIABLES OF *EXP* 2

Control Variables	NSGA-III	MFA	NSGA-FA	MOFA-PFA [14]
P_{G2}(MW)	41.7468	52.5462	52.6001	49.098
P_{G5}(MW)	33.4701	31.5729	29.4918	29.139
P_{G8}(MW)	34.8690	35.0000	35.0000	35.000
P_{G11}(MW)	26.0040	22.3209	20.7548	23.853
P_{G13}(MW)	17.5806	16.7236	17.5801	17.249
V_{G1}(p.u.)	1.0721	1.0806	1.1000	1.1000
V_{G2}(p.u.)	1.0602	1.0605	1.0919	1.0923
V_{G5}(p.u.)	1.0369	1.0371	1.0624	1.0631
V_{G8}(p.u.)	1.0481	1.0481	1.0726	1.0811
V_{G11}(p.u.)	1.0986	1.0974	1.0977	1.0714
V_{G13}(p.u.)	1.0761	1.0815	1.0972	1.0422
T_{11}(p.u.)	0.9402	1.0299	0.9680	1.0760
T_{12}(p.u.)	1.0706	0.9000	0.9833	0.9850
T_{15}(p.u.)	0.9919	0.9671	0.9845	1.0440
T_{36}(p.u.)	0.9622	0.9676	0.9785	1.0110
Q_{C10}(p.u.)	0.0025	0.0017	0.0487	0.0060
Q_{C12}(p.u.)	0.0245	0.0363	0.0059	0.0140
Q_{C15}(p.u.)	0.0086	0.0226	0.0153	0.0170
Q_{C17}(p.u.)	0.0171	0.0363	0.0489	0.0310
Q_{C20}(p.u.)	0.0425	0.0499	0.0292	0.0400
Q_{C21}(p.u.)	0.0055	0.0211	0.0258	0.0100
Q_{C23}(p.u.)	0.0294	0.0082	0.0362	0.0450
Q_{C24}(p.u.)	0.0241	0.0431	0.0402	0.0250
Q_{C29}(p.u.)	0.0056	0.0383	0.0195	0.0090
Fc_v ($/h)	869.84	867.60	**859.70**	860.37
Pl (MW)	5.9208	5.9195	**5.8620**	5.9547

B. Simulation on IEEE 57-bus System

A bi-objective and a tri-objective simulation experiments are carried out on the IEEE 57-bus system with complex structure. The high-dimensional MOOPF problems of large-scale system can evaluate the effectiveness of proposed NSGA-FA algorithm more comprehensively.

1) Exp 4: Simultaneous Optimization of Pl and Fc

The *Exp* 4 which takes *Pl* and *Fc* into account at the same time is simulated on the IEEE 57-bus system. Fig.7 shows the obtained PFs of *Exp* 4 while TABLE VII gives the control variables of BCS solutions. Fig.7 intuitively indicates the diversity and distribution of PFs obtained by MFA and NSGA-FA algorithms are more superior to NSGA-III method. Furthermore, the NSGA-FA method achieves the best PF with uniformly-distribution.

TABLE VII shows that the BCS of NSGA-FA which includes 11.4615 MW of *Pl* and 41876.43 $/h of *Fc* surpasses two BCS solutions found by NSGA-III and MFA algorithms.

TABLE VI
CONTROL VARIABLES OF *EXP* 3

Control Variables	NSGA-III	MFA	NSGA-FA	MODFA [24]
P_{G2}(MW)	58.5376	61.1514	63.9627	62.3246
P_{G5}(MW)	38.2504	35.1965	33.7187	40.1871
P_{G8}(MW)	34.9721	35.0000	34.8577	35.0000
P_{G11}(MW)	29.9978	28.5827	30.0000	30.0000
P_{G13}(MW)	29.1924	32.8397	31.1473	35.8428
V_{G1}(p.u.)	1.0471	1.0667	1.0966	1.0990
V_{G2}(p.u.)	1.0344	1.0505	1.0790	1.0880
V_{G5}(p.u.)	1.0164	1.0476	1.0537	1.0717
V_{G8}(p.u.)	1.0214	1.0350	1.0561	1.0838
V_{G11}(p.u.)	1.0512	1.0965	1.0449	1.0887
V_{G13}(p.u.)	1.0164	1.0566	1.0527	1.0953
T_{11}(p.u.)	1.0152	1.0518	1.0079	1.0384
T_{12}(p.u.)	1.0498	0.9347	0.9265	0.9261
T_{15}(p.u.)	1.0017	1.0160	0.9566	1.0146
T_{36}(p.u.)	1.0098	0.9647	0.9930	0.9627
Q_{C10}(p.u.)	0.0481	0.0292	0.0437	0.0304
Q_{C12}(p.u.)	0.0375	0.0324	0.0409	0.0464
Q_{C15}(p.u.)	0.0215	0.0347	0.0202	0.0412
Q_{C17}(p.u.)	0.0389	0.0450	0.0350	0.0445
Q_{C20}(p.u.)	0.0480	0.0481	0.0387	0.0363
Q_{C21}(p.u.)	0.0092	0.0053	0.0320	0.0328
Q_{C23}(p.u.)	0.0221	0.0404	0.0498	0.0312
Q_{C24}(p.u.)	0.0039	0.0420	0.0381	0.0324
Q_{C29}(p.u.)	0.0327	0.0284	0.0104	0.0130
Fc ($/h)	867.13	865.41	**863.79**	888.2006
Pl (MW)	4.7366	4.6916	**4.5558**	3.7487
Em (ton/h)	0.2133	0.2122	**0.2121**	0.2138

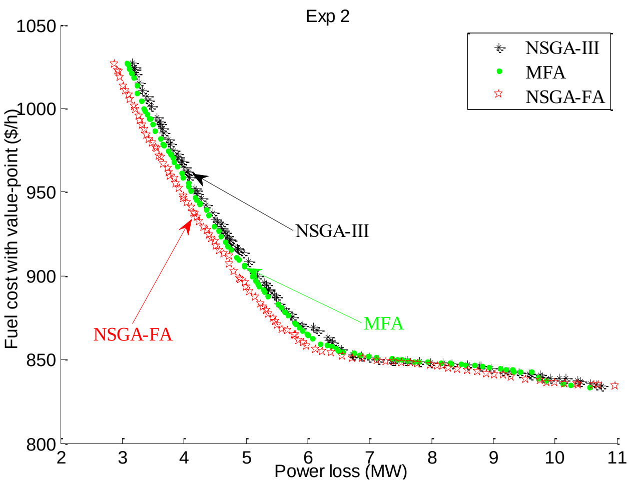

Fig.5. PFs of *Exp* 2

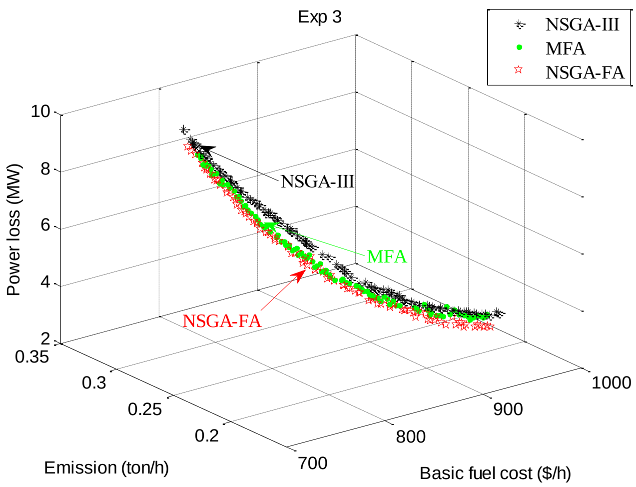

Fig.6. PFs of *Exp* 3

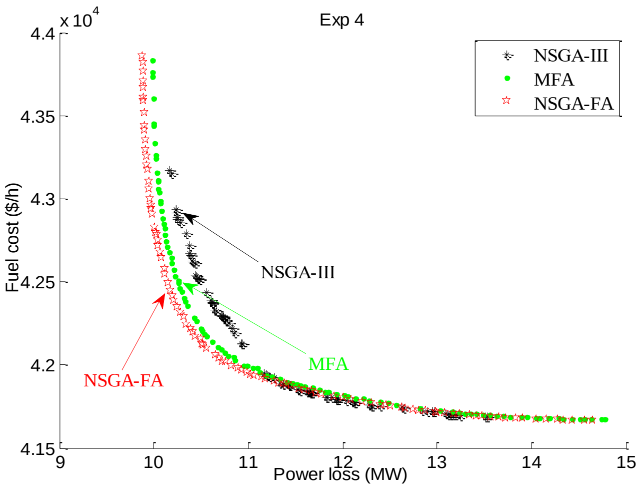

Fig.7. PFs of *Exp* 4

Besides, the suggested NSGA-FA algorithm is able to seek the more advantageous BCS solution in contrast to the published MOIBA and MOCS algorithms.

2) Exp 5: Simultaneous Optimization of Em, Pl and Fc

The *Exp* 5, a tri-objective case which optimizes *Em*, *Pl* and *Fc* simultaneously, is carried out to evaluate the quality of NSGA-FA algorithm. Fig. 8 shows the PFs of NSGA-III and NSGA-FA algorithms while Fig. 9 shows the PFs of MFA and NSGA-FA algorithms. Fig. 8 and Fig. 9 state that the PFs of NSGA-III and MFA methods are much more densely distributed than the novel NSGA-FA algorithm.

Meanwhile, the details of BCS solutions are given in TABLE VIII. It is not difficult to find that the BCS obtained by NSGA-FA algorithm including 1.3489 ton/h of *Em*, 12.2521 MW of *Pl* and 42666.00 $/h of *Fc* has dominant advantages than the ones of two mentioned comparison algorithms. The suggested NSGA-FA algorithm also achieves smaller *Fc* and *Em* values comparing with NSGA-II and MONBA-CPNS methods in literature [29], which further prove the great superiority of NSGA-FA in handling the tri-objective MOOPF problems.

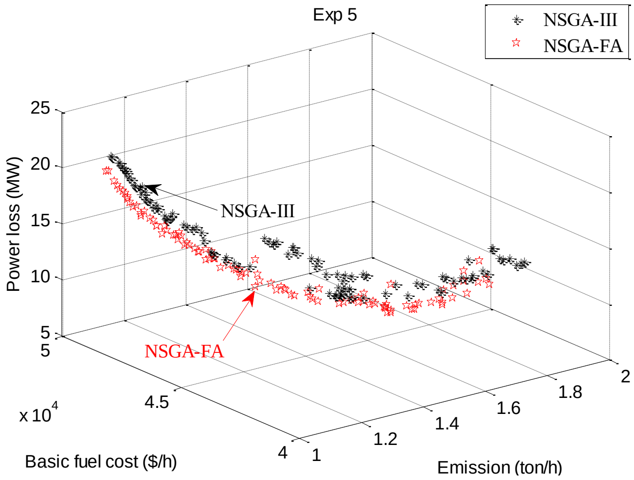

Fig.8. PFs of NSGA-III and NSGA-FA for *Exp* 5

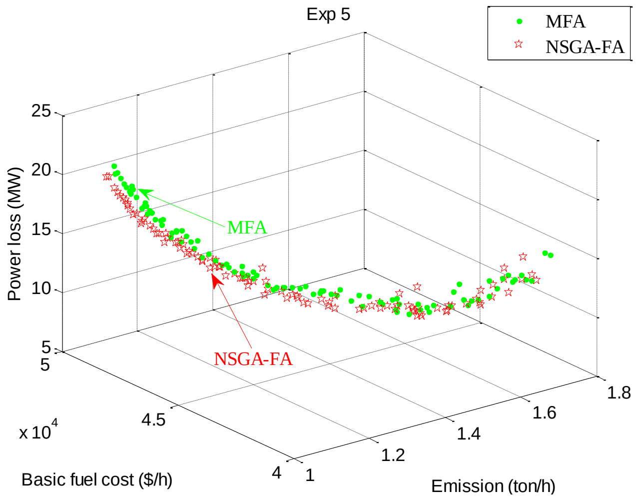

Fig.9. PFs of MFA and NSGA-FA for *Exp* 5

TABLE VII
CONTROL VARIABLES OF *EXP* 4

Control Variables	NSGA-III	MFA	NSGA-FA	MOCS [8]	MOIBA [18]
P_{G2}(MW)	63.4716	85.5006	89.3178	75.9674	53.4086
P_{G3}(MW)	56.6069	50.6662	47.6511	61.9222	62.6900
P_{G6}(MW)	97.6662	100.0000	100.0000	98.7284	89.8593
P_{G8}(MW)	380.5032	383.9519	381.5286	357.9396	377.9932
P_{G9}(MW)	99.8179	97.8913	96.7775	99.8737	99.9232
P_{G12}(MW)	410.0000	402.2013	398.6108	410.0000	410.0000
V_{G1}(p.u.)	1.0305	1.1000	1.1000	1.0251	1.0536
V_{G2}(p.u.)	1.0251	1.1000	1.1000	1.0217	1.0467
V_{G3}(p.u.)	1.0177	1.1000	1.1000	1.0165	1.0436
V_{G6}(p.u.)	1.0281	1.1000	1.1000	1.0142	1.0521
V_{G8}(p.u.)	1.0302	1.1000	1.1000	1.0072	1.0613
V_{G9}(p.u.)	1.0226	1.1000	1.1000	0.9889	1.0481
V_{G12}(p.u.)	1.0152	1.1000	1.1000	0.9961	1.0337
T_{19}(p.u.)	0.9311	0.9180	1.0671	1.0100	1.0350
T_{20}(p.u.)	0.9976	1.0793	0.9751	1.0800	0.9496
T_{31}(p.u.)	1.0205	1.0232	1.0356	1.0800	0.9837
T_{35}(p.u.)	0.9666	0.9000	0.9000	1.0400	1.0267
T_{36}(p.u.)	1.0995	1.1000	1.1000	0.9800	1.0055
T_{37}(p.u.)	0.9998	0.9936	1.0033	1.0300	1.0597
T_{41}(p.u.)	0.9278	1.0233	1.0261	0.9500	0.9682
T_{46}(p.u.)	0.9731	0.9255	0.9282	0.9700	0.9558
T_{54}(p.u.)	0.9389	1.0376	0.9160	0.9000	0.9893
T_{58}(p.u.)	0.9243	1.0171	0.9940	0.9400	0.9281
T_{59}(p.u.)	0.9194	1.0411	1.0216	0.9200	0.9192
T_{65}(p.u.)	0.9130	1.0326	1.0321	0.9400	0.9525
T_{66}(p.u.)	0.9002	1.0105	0.9980	0.9000	0.9441
T_{71}(p.u.)	0.9141	0.9684	0.9876	0.9200	0.9527
T_{73}(p.u.)	1.0746	1.0367	0.9769	1.0000	0.9421
T_{76}(p.u.)	0.9784	0.9479	0.9594	0.9800	1.0606
T_{80}(p.u.)	0.9346	1.0552	1.0440	0.9600	0.9688
Q_{C18}(p.u.)	0.2336	0.0028	0.0081	0.1700	0.2343
Q_{C25}(p.u.)	0.1771	0.1708	0.1536	0.1200	0.1310
Q_{C53}(p.u.)	0.0909	0.1270	0.1594	0.1600	0.1876
Fc ($/h)	41989.34	41885.48	**41876.43**	42176.1426	42098.72
Pl (MW)	11.5542	11.5106	**11.4615**	11.9950	11.4759

Therefore, the NSGA-FA algorithm proposed in this paper has significant advantages in solving the bi-objective and tri-objective MOOPF problems on IEEE 30-bus and 57-bus systems.

VI. EVALUATION

In order to make a comprehensive evaluation of the proposed NSGA-FA algorithm on MOOPF problems, the simulation results are analyzed based on the convergence, solution-diversity and computational-complexity.

A. Convergence

Take the *Exp* 2 which optimizes Fc_v and *Pl* on the IEEE 30-bus system as an example, the convergence of NSGA-III, MFA and NSGA-FA algorithms is studied. Fig. 10 shows the convergence of NSGA-FA and two comparison algorithms in the iterative process. It clearly indicates that NSGA-III and MFA methods implement the zero constraint-violation of each power flow solution at the 64th and 53th iterations, respectively. The presented NSGA-FA method realizes the zero constraint-violation at 41th iteration which verifies its advantages in fast-convergence.

TABLE VIII
CONTROL VARIABLES OF *EXP* 5

Control Variables	NSGA-III	MFA	NSGA-FA	NSGA-II [29]	MONBA-CPNS [29]
P_{G2}(MW)	97.5707	89.6198	84.8339	52.5225	99.1093
P_{G3}(MW)	96.3801	94.6345	85.4643	119.9929	97.7004
P_{G6}(MW)	97.2564	93.6857	94.3959	90.1155	89.4406
P_{G8}(MW)	365.8912	345.2355	350.2750	314.9157	312.8840
P_{G9}(MW)	99.5712	95.4810	99.6509	99.9551	98.3716
P_{G12}(MW)	364.2031	358.0269	349.0254	393.7500	404.5135
V_{G1}(p.u.)	1.0493	1.0894	1.0960	1.0708	1.0940
V_{G2}(p.u.)	1.0418	1.0881	1.0949	1.0608	1.0894
V_{G3}(p.u.)	1.0439	1.0837	1.0952	1.0438	1.0883
V_{G6}(p.u.)	1.0592	1.0820	1.0964	1.0303	1.0961
V_{G8}(p.u.)	1.0586	1.0835	1.0959	1.0249	1.0980
V_{G9}(p.u.)	1.0438	1.0811	1.0931	1.0293	1.0893
V_{G12}(p.u.)	1.0441	1.0780	1.0902	1.0348	1.0830
T_{19}(p.u.)	0.9657	1.0902	1.0715	0.9115	0.9756
T_{20}(p.u.)	1.0773	0.9924	1.0286	0.9706	1.0194
T_{31}(p.u.)	1.0114	1.0684	1.0627	1.0338	0.9533
T_{35}(p.u.)	1.0772	0.9113	1.0885	1.0472	1.1000
T_{36}(p.u.)	0.9291	1.0296	1.0298	1.0978	1.0631
T_{37}(p.u.)	1.0509	1.0386	0.9942	1.0522	0.9934
T_{41}(p.u.)	1.0606	1.0334	1.0036	0.9216	1.0238
T_{46}(p.u.)	1.0478	0.9983	0.9505	1.0156	0.9594
T_{54}(p.u.)	0.9483	0.9992	0.9251	0.9020	0.9938
T_{58}(p.u.)	0.9426	0.9902	0.9889	0.9360	0.9738
T_{59}(p.u.)	1.0037	0.9876	0.9913	0.9571	0.9791
T_{65}(p.u.)	0.9179	1.0313	0.9797	0.9277	0.9907
T_{66}(p.u.)	0.9884	0.9616	0.9721	0.9057	0.9709
T_{71}(p.u.)	0.9202	0.9816	1.0572	1.0070	1.0038
T_{73}(p.u.)	1.0584	1.0328	1.0614	1.0522	1.0997
T_{76}(p.u.)	1.0302	0.9814	0.9152	1.0067	0.9763
T_{80}(p.u.)	1.0023	1.0251	1.0260	0.9463	1.0077
Q_{C18}(p.u.)	0.2917	0.2955	0.1195	0.0989	0.1225
Q_{C25}(p.u.)	0.1953	0.1251	0.1502	0.1685	0.2179
Q_{C53}(p.u.)	0.2521	0.1359	0.1389	0.0898	0.1676
Fc ($/h)	42671.34	42816.49	**42666.00**	43931.30	43052.18
Pl (MW)	14.3596	12.3215	**12.2521**	11.2676	10.5961
Em (ton/h)	1.4090	1.3535	**1.3489**	1.4327	1.4292

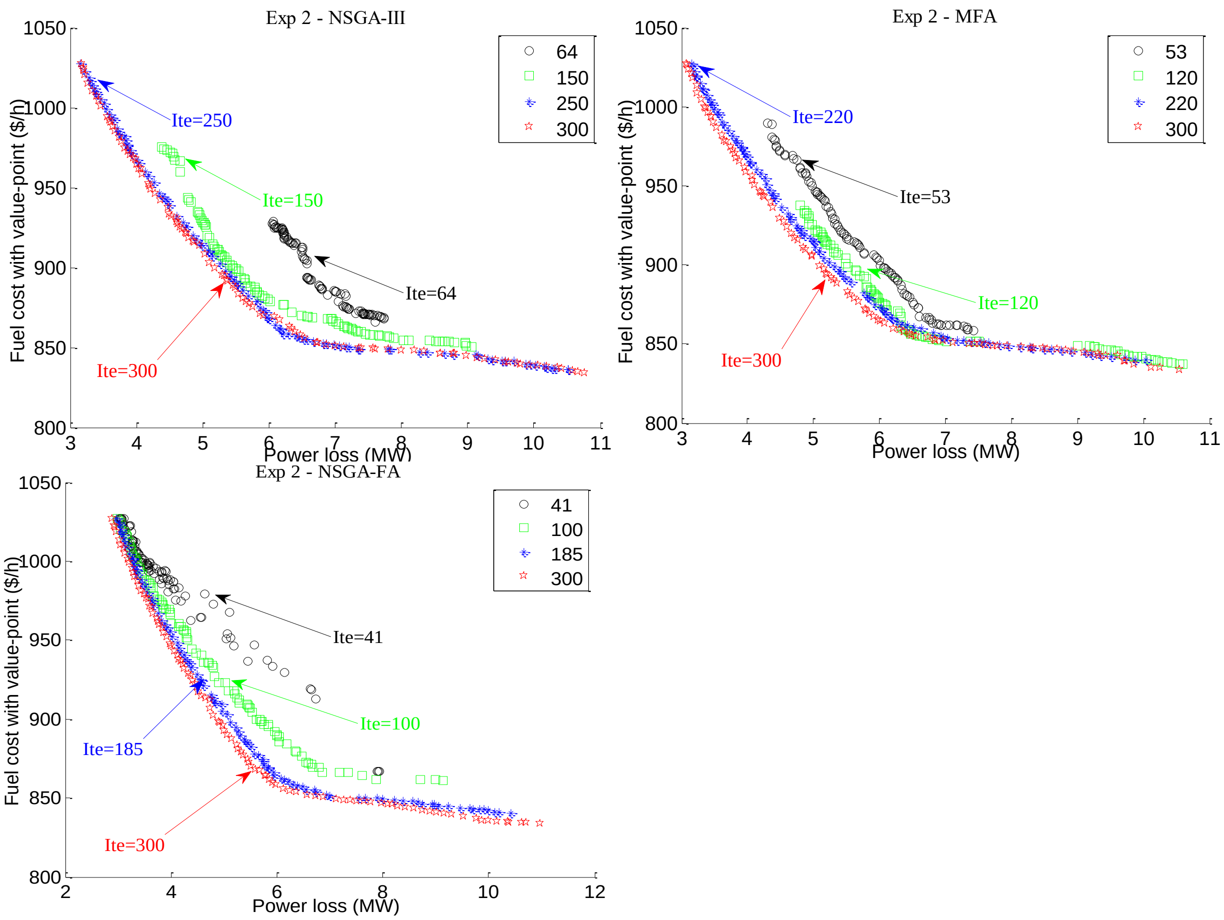

Fig.10. Convergence process of *Exp* 2

Furthermore, around the 250th and 220th iterations, NSGA-III and MFA algorithms find the evenly-distributed PFs. The NSGA-FA algorithm obtains the feasible PF with satisfactory distribution and diversity around the 185th iteration. The dynamic convergence process shown in Fig.10 directly proves the great superiority of NSGA-FA method in fast convergence.

B. Diversity

The hyper-volume (HV) index, the volume covered by obtained POS in the target space, is used to evaluate the solution-diversity of three mentioned algorithms [10, 24]. The HV indicator is defined as Formula (28). Generally, the larger the HV index, the better diversity of obtained POS.

$$HV = volume\left(\bigcup_{i=1}^{N} V_i\right) \tag{28}$$

where V_i is the volume covered by the ith power flow solution and reference points.

The boxplots of HV index in all bi-objective experiments are shown in Fig.11. Additionally, the average and standard deviation values are given in TABLE IX. The NSGA-FA algorithm obtains the larger HV average in *Exp* 1, *Exp* 2 and *Exp* 4, which represents that this proposed NSGA-FA method is more superior to NSGA-III and MFA algorithms in solution diversity.

In addition, the closer boxplots and smaller values of standard deviation clearly indicate that comparing with two mentioned comparison algorithms, NSGA-FA algorithm can realize the more stable and preferable operation state when dealing with MOOPF problems.

C. Complexity

Based on the running time of MATLAB program, the computational complexity of NSGA-III, MFA and NSGA-FA algorithms is analyzed. In detail, the running time of all simulation cases is summarized in TABLE X.

When handling the MOOPF problems, the computational complexity of NSGA-III algorithm is generally larger than the other two algorithms. Regrettably, the NSGA-FA algorithm requires more time cost and does not have obvious advantage on computational complexity compared to MFA algorithm. The optimization of NSGA-FA algorithm on reducing the computational complexity will be emphasized in the follow-up study.

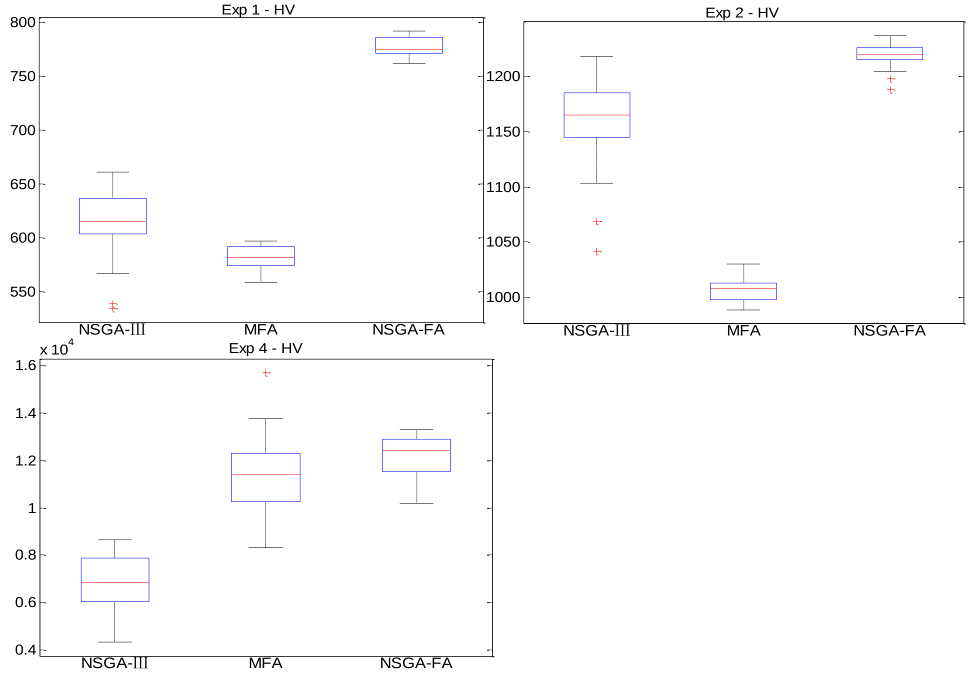

Fig.11. Boxplot of HV index for bi-objective experiments

TABLE IX
AVERAGE AND STANDARD DEVIATION OF HV INDEX

HV index		NSGA-III	MFA	NSGA-FA
Exp 1	average	612.73322	581.0839536	**776.6833917**
	standard deviation	31.0559723	10.31739302	8.342362851
Exp 2	average	1160.6190	1006.0829	**1218.7595**
	standard deviation	41.3918	10.5996	10.5867
Exp 4	average	6865.7760	11302.4262	**12202.6939**
	standard deviation	1113.4992	1649.2414	900.5869

TABLE X
RUNNING TIME OF ALL EXPERIMENTS

Time (*second*)	*Exp* 1	*Exp* 2	*Exp* 3	*Exp* 4	*Exp* 5
NSGA-III	154.8	167.0	187.9	516.9	529.2
MFA	146.3	159.1	173.2	504.1	518.5
NSGA-FA	148.6	165.3	179.7	512.4	522.6

VII. Conclusions

The presented NSGA-FA algorithm, the combination and improvement of NSGA-III and MFA algorithms in essential, is proposed to handle the non-convex MOOPF problems. The E_{-guide} mechanism and nonlinear ω_{non} coefficient integrated into NSGA-FA algorithm effectively optimize the global search ability and the diversity of potential solutions. To seek the satisfactory POS, the *NDES* storage strategy and the non-inferior sorting rule with constraints-violation are also put forward in this paper. The validness and excellence of the proposed NSGA-FA algorithm in contrast to NSGA-III and MFA algorithms are verified by five MOOPF trials. Furthermore, the comprehensive evaluation results such as HV index and convergence-analysis powerfully demonstrate the superiority of NSGA-FA algorithm in solution-diversity, fast-convergence and uniformity-distribution of PFs.

Therefore, the novel NSGA-FA algorithm provides another efficient method to solve the high-dimensional MOOPF problems and realizes the innovative application of computer technology in complex optimizations of power systems.

Acknowledgment

The authors appreciate the editors and reviewers for their constructive comments and suggestions.

References

[1] X. Yuan, B. Ji, Y. Yuan, R.M. Ikram, X. Zhang, and Y. Huang, "An efficient chaos embedded hybrid approach for hydro-thermal unit commitment problem", *Energy Conversion and Management*, vol. 91, pp. 225-237, 2015.

[2] Y. Jia, Z. Dong, C. Sun and K. Meng, "Cooperation-based distributed economic MPC for economic load dispatch and load frequency control of interconnected power systems", *IEEE Transactions on Power Systems*, vol. 34, no. 5, pp. 3964-3966, 2019.

[3] X. Yuan, Z. Chen, Y. Yuan, and Y. Huang, "Design of fuzzy sliding mode controller for hydraulic turbine regulating system via input state feedback linearization method", *Energy*, vol. 93, pp. 173-187, 2015.

[4] G. Chen, X. Yi, Z. Zhang, and S. Qiu, "Solving optimal power flow using cuckoo search algorithm with feedback control and local search mechanism", *IAENG International Journal of Computer Science*, vol. 46, no. 2, pp. 321-331, 2019.

[5] X. Yuan, B. Zhang, P. Wang, J. Liang, Y. Yuan, Y. Huang, and X. Lei, "Multi-objective optimal power flow based on improved strength Pareto evolutionary algorithm", *Energy*, vol. 122, pp. 70-82, 2017.

[6] G. Chen, J. Qian, Z. Zhang, and S. Li, "Application of modified pigeon-inspired optimization algorithm and constraint-objective sorting rule on multi-objective optimal power flow problem", *Applied Soft Computing*, vol. 92, pp. 10632, 2020.

[7] S. Khunkitti, A. Siritaratiwat, S. Premrudeepreechacharn, R. Chatthaworn, and N. R. Watson, "A hybrid DA-PSO optimization algorithm for multiobjective optimal power flow problems", *Energies*, vol. 11, no. 9, pp. 2270, 2018.

[8] G. Chen, S. Qiu, Z. Zhang, and Z. Sun, "Quasi-oppositional cuckoo search algorithm for multi-objective optimal power flow", *IAENG International Journal of Computer Science*, vol. 45, no. 2, pp. 255-266, 2018.

[9] J. Zhang, S. Wang, Q. Tang, Y. Zhou, and T. Zeng, "An improved NSGA-III integrating adaptive elimination strategy to solution of many-objective optimal power flow problems", *Energy*, vol. 172, pp. 945-957, 2019.

[10] G. Chen, J. Qian, Z. Zhang, and Z. Sun, "Applications of novel hybrid bat algorithm with constrained Pareto fuzzy dominant rule on multi-objective optimal power flow problems", *IEEE Access*, vol. 7, pp. 52060-52084, 2019.

[11] F. Wahid, R. Ghazali and L. H. Ismail, "Improved firefly algorithm based on genetic algorithm operators for energy efficiency in smart buildings", *Arabian Journal for Science and Engineering*, vol. 44, no. 4, pp. 4027-4047, 2019.

[12] G. Zhang, Y. Chen, Y. Li, H. Yu, H. Hu, and S. Wu, "Intelligent swarm firefly algorithm for the prediction of China's national electricity consumption", *International Journal of Bio-Inspired Computation*, vol. 13, no. 2, pp. 111-118, 2019.

[13] Huang, and Hsu-Chih, "A hybrid metaheuristic embedded system for intelligent vehicles using hypermutated firefly algorithm optimized radial basis function neural network", *IEEE Transactions on Industrial Informatics*, vol. 15, no. 2, pp. 1062-1069, 2019.

[14] G. Chen, X. Yi, Z. Zhang, and H. Lei, "Solving the multi-objective optimal power flow problem using the multi-objective firefly algorithm with a constraints-prior Pareto-domination approach", *Energies*, vol. 11, no. 12, pp. 3438, 2018.

[15] G. E. Manoranjitham and A. Shunmugalatha, "Multi-objective optimal power flow by placement of unified power flow controller using firefly algorithm", *Journal of Computational and Theoretical Nanoscience*, vol. 14, no. 12, pp. 6038-6043, 2017.

[16] G. Chen, Z. Lu, Z. Zhang, and Z. Sun, "Research on hybrid modified cuckoo search algorithm for optimal reactive power dispatch problem", *IAENG International Journal of Computer Science*, vol. 45, no. 2, pp. 328-339, 2018.

[17] S. Rahmani and N. Amjady, "Improved normalised normal constraint method to solve multi-objective optimal power flow problem", *IET Generation Transmission and Distribution*, vol. 12, no. 4, pp. 859-872, 2018.

[18] G. Chen, J. Qian, Z. Zhang, and Z. Sun, "Multi-objective improved bat algorithm for optimizing fuel cost, emission and active power loss in power system", *IAENG International Journal of Computer Science*, vol. 46, no. 1, pp. 118-133, 2019.

[19] M. Ding, H. Chen, N. Lin, S. Jing, F. Liu, X. Liang, and W. Liu, "Dynamic population artificial bee colony algorithm for multi-objective optimal power flow", *Saudi Journal of Biological Sciences*, vol. 24, no. 3, pp. 703-710, 2017.

[20] S. S. Reddy and P. R. Bijwe, "Differential evolution-based efficient multi-objective optimal power flow", *Neural Computing and Applications*, vol. 311, pp. 509-522, 2019.

[21] S. S. Reddy, "Optimal power flow using hybrid differential evolution and harmony search algorithm", *International Journal of Machine Learning and Cybernetics*, vol. 10, no. 5, pp. 1077-1091, 2019.

[22] A. Attia, R. A. El Sehiemy and H. M. Hasanien, "Optimal power flow solution in power systems using a novel Sine-Cosine algorithm", *International Journal of Electrical Power and Energy Systems*, vol. 99, pp. 331-343, 2018.

[23] X. S. Yang, S. S. S. Hosseini and A. H. Gandomi, "Firefly Algorithm for solving non-convex economic dispatch problems with valve loading effect", *Applied Soft Computing*, vol. 12, no. 3, pp. 1180-1186, 2012.

[24] G. Chen, X. Yi, Z. Zhang, and H. Wang, "Applications of multi-objective dimension-based firefly algorithm to optimize the power losses, emission, and cost in power systems", *Applied Soft Computing*, vol. 68, pp. 322-342, 2018.

[25] K. Deb, A. Pratap, S. Agarwal, and T. Meyarivan, "A fast and elitist multiobjective genetic algorithm: NSGA-II", *IEEE Transactions on Evolutionary Computation*, vol. 2, no. 6, pp. 182-197, 2002.

[26] H. Li, K. Deb, Q. Zhang, P. N. Suganthan, and L. Chen, "Comparison between MOEA/D and NSGA-III on a set of novel many and multi-objective benchmark problems with challenging difficulties", *Swarm and Evolutionary Computation*, vol. 46, pp. 104-117, 2019.

[27] P. C. Roy, K. Deb and M. M. Islam, "An efficient nondominated sorting algorithm for large number of fronts", *IEEE Transactions on Cybernetics*, vol. 49, no. 3, pp. 859-869, 2019.

[28] G. Chen, J. Qian, Z. Zhang, and Z. Sun, "Multi-objective optimal power flow based on hybrid firefly-bat algorithm and constraints-prior object-fuzzy sorting strategy", *IEEE Access*, vol. 7, pp. 139726-139745, 2019.

[29] G. Chen, J. Qian, Z. Zhang, and Z. Sun, "Many-objective new bat algorithm and constraint-priority non-inferior sorting strategy for optimal power flow", *Engineering Letters*, vol. 27, no. 4, pp. 882-892, 2019.